Evaluation of the MASW technique in unconsolidated sediments

Jianghai Xia, Richard D. Miller, and Choon B. Park, Kansas Geological Survey;*
James A. Hunter, Geological Survey of Canada; James B. Harris, Millsaps College

Summary

Shear (S) wave velocities derived from the MASW (multi-channel analysis of surface wave) technique and borehole measurements at seven well locations in unconsolidated sediments of the Fraser River Delta are compared. The overall difference between these two sets of S-wave velocities is about 15%. S-wave velocities from the MASW technique at an additional location are also obtained and await comparison with borehole measurements.

Introduction

The Kansas Geological Survey and the Geological Survey of Canada conducted a test project of a surface wave technique (Park et al., 1999; Xia et al., in press) in the Fraser River Delta, Vancouver, Canada from October 3 to October 8, 1998. A thorough study of S-wave velocities in this area has been done previously (Hunter et al., 1998). Vertical profiles of S-wave velocity based on borehole measurements are available in more than 30 locations. These S-wave velocity profiles provide the ground truth of S-wave velocity in this area. Eight sites were selected based on geographic location, accessibility and availability of boreholes, and the pattern of S-wave velocity from borehole measurements. Table 1 lists all boreholes included in this project. One borehole, for which S-wave velocities from borehole measurements were not available during the surface-wave processing period, is labeled as "unknown."

Data Acquisition

Multi-channel surface wave data were acquired by 60 (or 48) 4.5 Hz vertical component geophones and a Geometrics StrataView seismograph. Sixty (or 48) geophones were deployed on 0.6 (or 1.2) meter interval with the nearest source-to-geophone offset in the range of 1.2 meters to 90 meters. The seismic source was a weight dropper built by the Exploration Services Section of the Kansas Geological Survey. Three to ten impacts were vertically stacked at each offset. No acquisition filter was applied during data acquisition. The record length is 2048 milliseconds with a 1 millisecond sample interval. At boreholes FD92-3 and "Unknown," the seismograph was manually triggered due to interference of an electromagnetic field. The first breaks in these two sites are not correctly related to source-geophone offsets. Fortunately, the first break is not necessary to extract Rayleigh wave phase velocities from a shot gather.

Table 1. Field parameters in data acquisition.

Borehole ID (figure #)	Field-record number	Number of channels	Nearest offset (m)	Geophone spacing (m)	Longest wavelength observed (m)	Shortest wavelength observed (m)	Phase velocity range observed (m/s)	Frequency range observed (Hz)
FD95-2 (1)	3060	48	9	0.6	22.6	5.7	130–158	7–23
FD97-2 (2)	275	60	18	1.2	56.4	6.5	127–169	3–19.5
FD92-11	1059	60	18	0.6	44.2	3.2	85–176	4–27
FD92-3 (3a)	3031	60	Arbitrary*	0.6	109.5	4.8	93–328	3–19.5
Unknown (3d)	4040	60	Arbitrary*	0.6	59.7	7.2	107–180	3–14.8
FD86-5 (3b)	5015	60	18	0.6	29.3	3.9	99–146	5–25
FD92-4	6011	60	18	0.6	68.3	3.8	96–239	3.5–25
FD97-7 (3c)	7035	60	4.8	0.6	31.3	4.2	29–63	2–7

**The actual nearest offset for cases FD92-3 and Unknown are 16.8 m. The reason of using "Arbitrary" in this column is that the seismograph is manually triggered due to interference of an electromagnetic field in the testing areas. The first breaks in these two records are not correctly related to the source-geophone offset.*

Data Processing

Multi-channel surface wave data were processed by SurfSeis, a proprietary set of algorithms developed by the Kansas Geological Survey. The theory on which SurfSeis is based can be found in Park et al. (1999) and Xia et al. (in press). At the present time, the software can only be used to process fundamental-mode Rayleigh waves.

Evaluation of the MASW technique

Our experience shows that the optimum nearest offset is in the range of one half to one of the depth of interest. Within this range, the ratio of energy of surface waves components for the interested depth to energy of body waves could be the highest. In order to keep comparison consistent, shot gathers that were processed to provide S-wave velocity profiles are associated with the nearest offset in the range of about 10 to 20 meters. The extreme case is borehole FD97-7. The shot gather that was used to provide the S-wave velocity profile has a nearest offset of 4.8 meters. This is because the Rayleigh wave phase velocity is extremely low (29–63 m/s). The recording time we chose for farther offsets is not long enough to record the entire Rayleigh wave.

Table 1 lists basic information about shot gathers in all sites used to calculate S-wave velocity profiles in the order that the data were acquired. The frequency contents of the Rayleigh wave phase velocities are roughly in the range of 5 to 25 Hz. The shortest wavelength observed is in the range of 4 to 7 meters. The longest wavelength, however, changes in a broad range that is mainly affected by S-wave velocities of relatively deeper layers.

Rayleigh wave phase velocity at a specific frequency (dispersion data) is the function of four parameters: S-wave velocity, compressional (P) wave velocity, density, and layer thickness. S-wave velocity is the dominant influence on the Rayleigh wave phase velocity. In our inversion method (Xia et al., in press) only the S-wave velocity is modified after each iteration. P-wave velocity is "blindly" determined by a fixed Poisson's ratio (0.45) in all cases. Density is also predetermined by fixing to 2.0 g/cm^3 for all layers. The thickness of layers is set to two meters for all cases except borehole FD97-7, for which it is one meter.

Errors in selected P-wave velocity and density will definitely be introduced into inverted S-wave velocities. Based on Xia et al.'s results (in press), 25% error in P-wave velocity and the same percent error in density will convert with less than 7% error to inverted S-wave velocities.

The MASW technique derives S-wave velocities for a layered Earth model by inverting Rayleigh wave phase velocities (the dispersion curve). The root-mean-square error between measured phase velocity and calculated phase velocity based on the inverted S-wave velocity model (Figures 1–3) are in the range of 1–4 m/s. Initial S-wave velocity models are automatically determined by SurfSeis. SurfSeis guarantees convergence based on initial values calculated by the software itself (Xia et al., in press). Inverted models (Figures 1c, 2c, and 3) are obtained in around ten iterations in less than two minutes on today's Pentium desktop computer. Depths of S-wave velocities from borehole measurements (Hunter et al., 1998) are usually much deeper than what are shown in Figures 1c, 2c, and 3. We plot only a shallower portion where S-wave velocities from the MASW technique are available to be compared.

Discussions

We used six different criteria to describe the difference between S-wave velocities from borehole measurements and the MASW technique: the maximum difference, average difference, the maximum relative difference, average relative difference, standard deviation, and relative standard deviation. See Table 2 for mathematical expressions of these criteria.

Table 2. Comparison inverted S-wave velocity with borehole results.

Borehole ID (figure #)	Maximum difference (m/s)	Average difference (m/s)	Maximum relative difference (%)	Average relative difference (%)	Standard deviation (m/s)	Relative standard deviation (%)	Depth studied by MASW (m)	Inverted velocity range(m/s)
FD95-2 (1)	35.8 at 24 m	19.0	17.7 at 8 m	10.2	15.5	9.8	30	111–206
FD97-2 (2)	50.8 at 2 m	15.9	31.3 at 2 m	9.1	13.8	8.7	30	111–207
FD92-11	46.6 at 20 m	24.4	32.4 at 6 m	15.2	19.7	12.0	30	91–237
FD92-3 (3a)	157.4 at 26 m	42.0	39.8 at 4 m	17.2	42.0	17.3	30	82–404
Unknown (3d)							30	126–200
FD86-5 (3b)	94.8 at 17.5 m	49.5	42.9 at 10 m	25.8	40.1	28.2	30	98–186
FD92-4	60.2 at 20 m	18.8	32.8 at 20 m	10.4	18.0	8.9	30	92–311
FD97-7 (3c)	33.4 at 7 m	21.6	370 at 2 m	135	16.6	34.6	7	29–67

Terminology used in this table:
The maximum difference $D = \max_{1 \le j \le n} |V_b - V_i|_j$, *where* V_b *is S-wave velocities from borehole measurement,* V_i *is S-wave velocities inverted from Rayleigh wave phase velocities, and n is the number of layers. Average difference* $\underline{D} = \frac{1}{n}\sum_{k=1}^{n}\left|V_b - V_i\right|_k$. *The maximum relative difference*

$R = 100*D/(V_b)_k$, where $(V_b)_k$ is the S-wave velocity from borehole measurement associated with D. Average relative difference $\underline{R} = \frac{100}{n}\sum_{k=1}^{n}(|V_b - V_i|/V_b)_k$ *Standard deviation* $S = \sqrt{\frac{1}{2n}\sum_{k=1}^{n}(V_b - V_i)_k^2}$. *Relative standard deviation = ratio of S to the median of the inverted velocities (in column nine).*

The maximum difference shows the greatest difference between S-wave velocities from borehole measurements and MASW results. In the second column of Table 2, for example, the maximum difference for borehole FD92-3 (Figure 3a) is 157.4 m/s at depth 26 meters. This actually is the biggest difference in the seven boreholes.

The average difference in column three of Table 2 is an arithmetic average of the difference between two results. For example, it is 42.0 m/s for borehole FD92-3 (Figure 3a).

The maximum relative difference is the ratio of the maximum difference to the borehole measurement at the same depth. The depth associated with the maximum difference and maximum relative difference may not be the same. For example, for borehole FD92-3 (Figure 3a) the maximum relative difference is 39.8% at a depth of 4 meters rather than at 26 meters of depth.

The average relative difference in column five of Table 2 is an arithmetic average of the relative difference of all layers. It is 17.2% for borehole FD92-3 (Figure 3a). This criterion describes an overall difference between S-wave velocities from borehole measurements and MASW results. We may claim that the overall difference between two results is about 15% if results for borehole FD97-7 (Figure 3c) are excluded. A huge difference appears in the case of borehole FD97-7 (Figure 3c). Near-surface geology (peat) at borehole FD97-7 provides a challenge to the MASW technique. An extremely low velocity is observed in our field data. Dispersion data extracted from the shot gather indicate the lowest phase velocity is 29 m/s. The lowest inverted S-wave velocity is 29 m/s. However, based on borehole measurements, S-wave velocity at the surface is only 7 m/s so that a relative difference of more than 300% occurs at the shallowest part of the depth-velocity profile.

Column six shows the standard deviation. This criterion tells us pretty much the same story as the relative difference does when a ratio (column seven) of the standard deviation to the median of column nine is calculated. Using FD95-2 (Figure 1) as an example, the median of the inverted velocities (column nine) is 158.5 m/s so that the ratio of standard deviation to the median is 9.8% (=15.5/158.5).

We may classify S-wave velocities obtained by the MASW technique into three groups: 1. *Excellent agreement*. Inverted S-wave velocities by the MASW technique match almost perfectly with borehole measurements. They are FD95-2 (Figure 1), FD97-2 (Figure 2), and FD92-4. The average relative difference (column five of Table 2) between the two results in this group is about 10%. 2. *Good agreement*. There is a big difference in only one layer. They are FD92-11 at a depth of 6 m and FD92-3 (Figure 3a) at a depth of 26 m. Inverted S-wave velocities by the MASW technique could fall into the first category if this one layer S-wave velocity is not used to calculate differences. 3. *Fair agreement*. Bigger differences (more than 20%) between both results occur in more than one layer. They are FD86-5 (Figure 3b) and FD97-7 (Figure 3c). Although the differences in S-wave velocity in these two boreholes are obvious, a general trend of S-wave velocities for both results is still consistent to a certain degree.

Acknowledgments

The authors would like to thank Brett Bennett David Laflen, Ron Good, Jim Droddy, and Chad Gratton for their assistants during the field tests. The authors appreciate the efforts of Mary Brohammer, John Charlton, and Amy Stillwell in the manuscript and slide preparations.

References

Hunter, J.A.M., Burns, R.A., Good, R.L., and Pelletier C.F., 1998, A compilation shear wave velocities and borehole geophysical logs in Unconsolidated sediments of the Fraser River Delta: Geological Survey of Canada, Open File No. 3622.

Park, C.B., Miller, R.D., and Xia, J., 1999, Multi-channel analysis of surface waves (MASW): *Geophysics*, May-June issue.

Xia, J., Miller, R.D., and Park, C.B., in press, Estimation of near-surface shear wave velocity by inversion of Rayleigh waves: *Geophysics*.

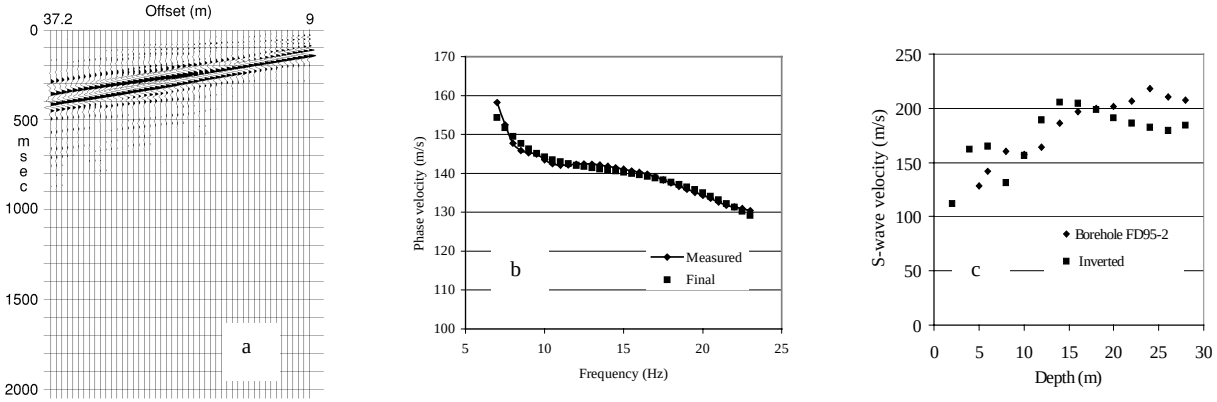

Fig.1. Field shot gather (a) with 48 traces at location of borehole FD95-2, Rayleigh wave phase velocities (b) extracted from (a) labeled Measured, and from inverted Vs model (c) labeled Final.

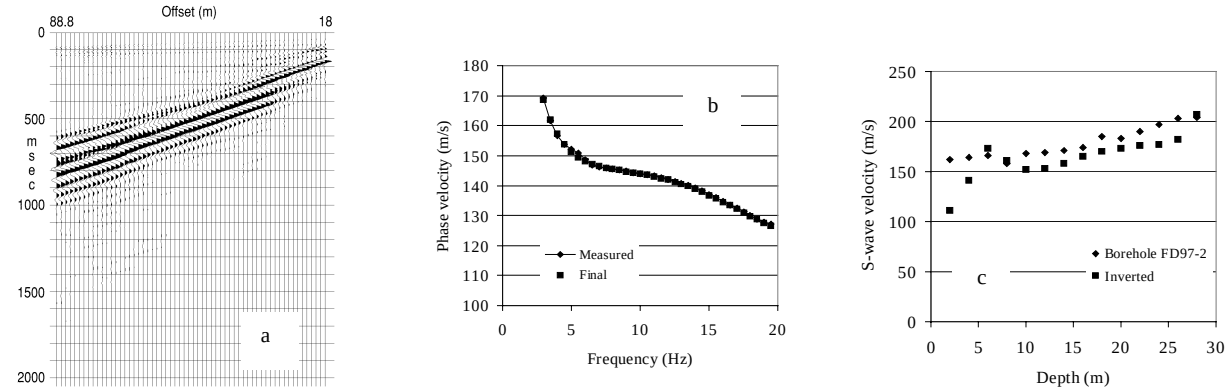

Fig. 2. Field shot gather (a) with 60 traces at location of borehole FD97-2, Rayleigh wave phase velocities (b) extracted from (a) labeled Measured, and from inverted Vs model (c) labeled Final.

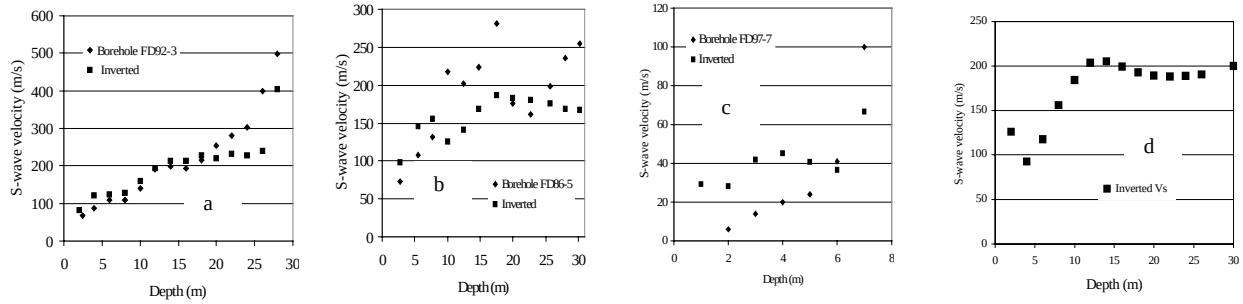

Fig. 3. Inverted S-wave velocities and borehole measurements for well FD92-3 (a), FD86-5 (b), FD97-7 (c), and the "unknown" well (d).

This article has been cited by:

1. Julian Ivanov, Richard Miller, Shelby PeterieDetecting and delineating voids and mines using surface-wave methods in Galena, Kansas 2344-2350. [Abstract] [References] [PDF] [PDF w/Links]
2. Julian Ivanov*, Richard D. Miller, Shelby L. Peterie, Robert F. BallardJr., Joseph B. DunbarRevisiting levees in southern Texas using Love-wave multi-channel analysis of surface waves (MASW) with the high-resolution linear radon transform (HRLRT) 2211-2217. [Abstract] [References] [PDF] [PDF w/Links]
3. Julian Ivanov, Richard D. Miller, Sarah Morton, Shelby PeterieDISPERSION-CURVE IMAGING CONSIDERATIONS WHEN USING MULTICHANNEL ANALYSIS OF SURFACE WAVE (MASW) METHOD 556-566. [Abstract] [References] [PDF]
4. Julian Ivanov*, Richard D. Miller, Shelby L. Peterie, Georgios TsofliasNear-surface Qs and Qp estimations from Rayleigh waves using multi-channel analysis of surface waves (MASW) at an Arctic ice-sheet site 2006-2012. [Abstract] [References] [PDF] [PDF w/Links]
5. Julian Ivanov, J. Tyler Schwenk, Richard D. Miller, Shelby PeterieDispersion-curve imaging nonuniqueness studies from multi-channel analysis of surface waves (MASW) using synthetic seismic data 1794-1800. [Abstract] [References] [PDF] [PDF w/Links]
6. Julian Ivanov, Richard D. Miller, Shelby Peterie, Chong Zeng, Jianghai Xia, Tyler SchwenkMulti-channel analysis of surface waves (MASW) of models with high shear-wave velocity contrast 1384-1390. [Abstract] [References] [PDF] [PDF w/Links]
7. Julian Ivanov, Richard D. Miller, Jianghai Xia, Shelby PeterieMulti-mode inversion of multi-channel analysis of surface waves (MASW) dispersion curves and high-resolution linear radon transform (HRLRT) 1902-1907. [Abstract] [References] [PDF] [PDF w/Links] [Supplemental Material]
8. Julian Ivanov, Carole D. Johnson, John W. Lane, Richard D. Miller, Drew ClemensNear-surface evaluation of Ball Mountain Dam, Vermont, using multi-channel analysis of surface waves (MASW) and refraction tomography seismic methods on land-streamer data 1454-1458. [Abstract] [References] [PDF] [PDF w/Links]
9. Julian Ivanov, Richard D. Miller, Richard D. Markiewicz, Jianghai XiaRefraction tomography mapping of near-surface dipping layers using landstreamer data at East Canyon Dam, Utah 3229-3233. [Abstract] [References] [PDF] [PDF w/Links] [Supplemental Material]
10. Julia Ivanov, Richard D. Miller, Jianghai Xia, Joseph B. DunbarApplications of the JARS method to study levee sites in southern Texas and southern New Mexico 1725-1729. [Abstract] [References] [PDF] [PDF w/Links]